Ain Shams Engineering Journal (2015) 6, 403–411

Ain Shams University

Ain Shams Engineering Journal

www.elsevier.com/locate/asej
www.sciencedirect.com

CIVIL ENGINEERING

Investigating the effect of curved shape of bridge abutment provided with collar on local scour, experimentally and numerically

Y. Abdallah Mohamed [a,*], T. Hemdan Nasr-Allah [b], G. Mohamed Abdel-Aal [a], A. Shawky Awad [b]

[a] Zagazig University, Faculty of Engineering, Egypt
[b] Benah University, Faculty of Engineering, Egypt

Received 29 April 2014; revised 12 October 2014; accepted 17 October 2014
Available online 6 December 2014

KEYWORDS

Numerical models;
Hydraulic structure;
Abutment shape;
Bridge abutments;
Local scour;
SSIIM

Abstract Scour around bridge supports such as abutments can result in structural collapse and loss of life and property, so there is a need to control and minimize the local scour depth. In this paper, numerical and experimental studies were carried out to investigate the effect of different relative radii of the bridge abutment provided with collar on local scour depth. A 3-D numerical model is developed to simulate the scour at bridge abutment using SSIIM program. This model solves 3-D Navier–Stokes equations and a bed load conservation equation. The k–ε turbulence model is used to solve the Reynolds-stress term. It was found the curvature shape of bridge abutment provided with collar could share to reduce the local scour depth by more 95%. In addition, the results of simulation models agree well with the experimental data.

1. Introduction

Local scour at bridge foundation can cause damage or failure of bridges and result in excessive repairs, or even death. A study was produced in 1973 for the U.S. Federal Highway Administration that concluded of 383 bridge failures, 25% involved pier damage and 72% involved abutment damage [1]. There are generally three types of scours that affect the performance and safety of bridges, namely, local scour, contraction scour, and degradational scour [2]. Scour countermeasures can be generally categorized into two groups: armoring countermeasures and flow altering countermeasures. The armoring countermeasure is the addition of another layer, to resist the hydraulic shear stress and therefore provides protection to the erodible materials underneath. In the other side, the flow altering countermeasures aim to change the hydraulic properties of flows by using spur dikes, guide banks, parallel walls, collars, etc., and therefore reducing the scour effect at bridge piers and abutments [3]. A comprehensive review of different scour countermeasures for bridge piers

* Corresponding author.
E-mail addresses: Yasser_eng1997@zu.edu.eg, Yasser_eng1997@yahoo.com, ymoussa@jazanu.edu.sa (Y.A. Mohamed).
Peer review under responsibility of Ain Shams University.

Production and hosting by Elsevier

http://dx.doi.org/10.1016/j.asej.2014.10.011

and abutments was investigated [4,5]. Spur dikes as a countermeasure to local scour at wing wall abutments was studied experimentally [6]. There are different methods for estimating local scour depth at bridge abutments [7–10]. In addition, lots of researches are carried out to minify the scour dimensions by implementing a circular collar around the pier [11–16], submerged vanes [17], a slot through the pier [18–22]. The guide wall was used to protect the scour depth at bridge abutment [23]. The effect of constructing two adjacent bridges on the flow characteristics and local scour around bridge piers was discussed [24]. Integrating approach to the estimation of local scour depth at bridge piers and abutments was presented [25]. Scour around bridge abutment is studied experimentally [26–28]. Bridge abutment was studied numerically [29,30]. Analysis of experimental data sets for local scour depth around bridge abutments using artificial neural networks was investigated [31]. Gene expression programming and artificial neural networks were used to predict the time variation of scour depth at a short abutment [32]. Previous studies [33,34] showed that different empirical equations may predict various bridge scour depths for a certain case. Hence, numerical simulation of local scour depth may be assumed as an alternative and to some extent more reliable scour depth predictor. Another important issue in the estimation of bridge scour depth deals with scale effect [35]. In fact, traditional methodologies originally developed on the basis of small-scaled laboratory experiments, while this problem will not be faced in numerical simulations. In the present study, the scour depth at bridge abutment has curved shape and provided with collar was studied numerically and experimentally. The simulated models were created by using SSIIM (sediment simulation in water intakes with multiblock option) program. This 3D CFD model was based on the finite volume method to solve the Navier–Stokes equations [36].

2. Experimental work

The experimental work was carried out in a re-circulating channel with 4 m length, 20 cm depth and 40 cm width (Photo 1). Stones with different sizes were used at entrance to damp carefully disturbances. The discharge was measured using a pre-calibrated orifice meter. The median sand size (D_{50}) is 1.77 mm. The sediment is to be considered as uniform at which the geometric stander deviation of the particle size distribution is less than 1.3 ($\sigma_g = D_{84}/D_{50\ =\ 1.29}$). The experimental work was conducted under the clear-water condition. Clear water scour occurs for velocities up to the threshold for the general bed movement, i.e., $U/U_c \leqslant 1$ (U, is the approach flow velocity, and U_c, is mean approach velocity at the threshold condition [25]. In the present study the value of U/U_c equals 0.86 (i.e., clear water scour). For each test of the experimental program, the sand was leveled along the entire length of flume using a wooden screed with the same width as the flume. The sand level was checked in random points with a point gauge. The flume was slowly filled with water to the required depth. The pump was then turned on and its speed increased slowly until the desired flow rate was achieved, after that the tailgate was adjusted to get the required water depth. At the end of the test the pump was turned off and the flume was drained slowly without disturbing the scour topography. The bed topography was measured with point gauge with 0.01 mm accuracy on a grid with meshes of 3 cm × 3 cm (sometimes 1 cm × 1 cm depending on the bed topography) over an area of 2.5 m × 0.4 m spanning between 1.0 m upstream and 1.1 m downstream from the abutment. The grid pattern was dense to obtain accurate bed topography at the end of each experiment. Details of experimental models were shown in Fig. 1. Wooden edge abutments with 40 cm length (L), and 7.5 cm widths (b), were installed in the channel sides. The used protective plate (collar) in the experiments is 2 mm thickness and is made from Perspex. The collars fixed at the same level as the mobile bed. The collar width (L_1), is 6 cm, and the collar lengths (L_c), are ranged from 29 to 59 cm. The curvature radii (r) are 1.5, 3, 4.5, 6, 7.5, 9, 10.5, 18.15, 30.5 and 100 cm. The total numbers of experiments are 80. Details of the experimental conditions were summarized in Table 1. Fig. 2, presents the required time for each test, in which $d_s/d_{s\text{Equilibrium}}$ was plotted against the time. It was found that 90% of maximum scour depth was achieved at 2 h.

3. The numerical model

The SSIIM program solves the Navier–Stokes equations with the k–ε on a three dimensional and general non-orthogonal co-ordinates. These equations are discretized with a control volume approach. An implicit solver is used, producing the velocity field in geometry. The velocities are used when solving the convection–diffusion equations. The Navier–Stokes equations for non-compressible and constant density flow can be modeled as follows:

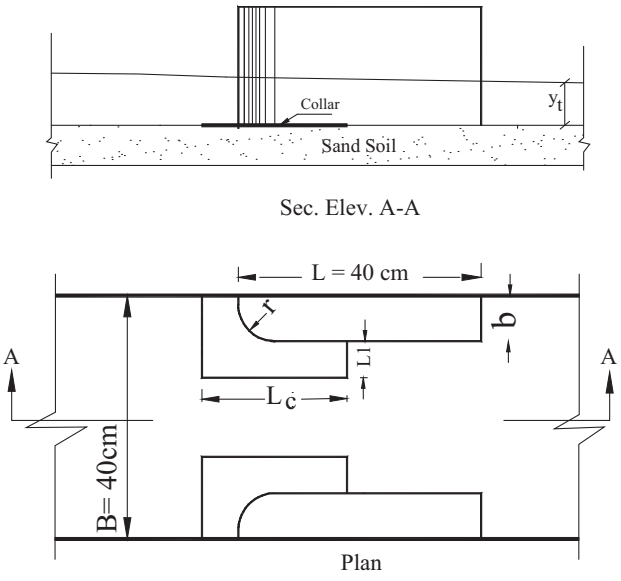

Figure 1 Sketch of experimental models.

Table 1 Details of experimental conditions.

Discharge (L/s)	3.5	Median sand size (mm)	1.77
Abutment width (b) cm	7.5	Flow depth (cm)	3–7
Collar width (L_1) cm	6	Froude number	0.20–0.55
Collar length (L_c) cm	29–58	Radius (r) cm	1.5–100

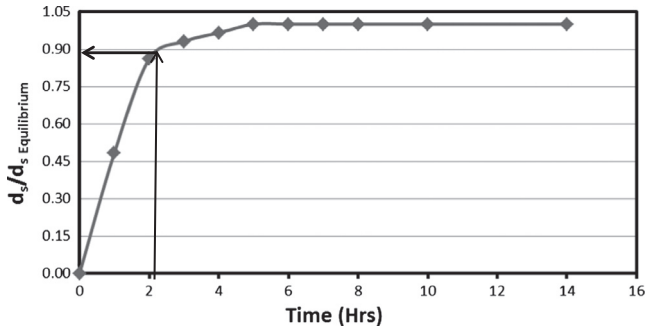

Figure 2 Ratio of maximum to equilibrium scour depths ($d_s/d_{sEquilibrium}$) versus time.

$$\frac{\partial u_i}{\partial t} + U_j \frac{\partial u_i}{\partial x_j} = \frac{1}{\rho} \frac{\partial}{\partial x_j} \left[-p\delta_{ij} - \rho \overline{u_i u_j} \right] \tag{1}$$

The left term on the left side of the Eq. (1) indicates the time variations. The next term is the convective term. The first term on the right-hand side is the pressure term and the second term on the right side of the equation is the Reynolds stress. The Reynolds stress is evaluated using turbulence model k–ε. The free surface is calculated using a fixed-lid approach, with zero gradients for all variables. The locations of the fixed lid and its movement as a function of time and water flow field are computed by different algorithms. The 1D backwater computation is the default algorithm and it is invoked automatically. Formula developed by Van Rijn [37] was used to calculate the equilibrium sediment concentration close to the bed. This equation has the form

$$C_{\text{bed}} = 0.015 \frac{d^{0.3}[(\tau - \tau_c)/\tau_c]^{1.5}}{a[((\rho_s - \rho_w)g)/(\rho_w v^2)]^{0.1}} \tag{2}$$

where C bed is the sediment concentration, d is the sediment particle diameter, a is a reference level set equal to the roughness height, τ is the bed shear stress, τ_c is the critical bed shear stress for movement of sediment particles according to Shield's curve, ρ_w and ρ_s are the density of water and sediment respectively, v is the Kinematic viscosity of the water and g is the gravitational acceleration.

The bed load discharge (q_b) can be calculated using the following equation [37]:

$$\frac{q_b}{D_{50}^{1.5}\sqrt{((\rho_s - \rho_w)g)/\rho_w}} = 0.053 \times \frac{d^{0.3}[(\tau - \tau_c)/\tau_c]^{1.5}}{D_{50}^{0.3}[((\rho_s - \rho_w)g)/(\rho_w v^2)]^{0.1}} \tag{3}$$

where D_{50} is the mean size of sediment.

The influence of rough boundaries on fluid dynamics is modeled through the inclusion of the wall law

$$\frac{U}{U_*} = \frac{1}{K} \ln(30z/K_s) \tag{4}$$

where k_s equals to the roughness height, K is von Karmen constant, U is the mean velocity, U_* is the shear velocity and z is the height above the bed.

4. Model geometry and properties

A structured grid mesh on the x–y–z plane was generated: three dimensional grid mesh with 234 elements in the x-direction, 66 elements in the y-direction and 22 elements in the z-direction. An uneven distribution of grid lines in both horizontal and vertical directions was chosen in order to keep the total number of cells in an acceptable range and to get valuable results in the area. The following grid line distributions were chosen: In X-direction: 3 cells with a 0.25 m, 10 cells with a 0.05 m, 25 cells with a 0.02 m, 160 cells with a 0.005 m, 20 cells with a 0.02 m, 10 cells with a 0.05 m and 5 cells with a 0.11 m respectively. In Y-direction: 30 cells with a 0.005 m, 5 cells with a 0.02 m and 30 cells with a 0.005 m respectively. In Z-direction: 10 cells with 1% height of the water depth, 4 cells with 5% of the water depth and 7 cells with 10% of the water depth. The Abutment was generated by specifying its ordinates, and then the grid interpolated using the elliptic grid generation method. However, the Abutment was generated by blocking the area of the Abutment.

5. Analysis and discussion

5.1. Effect of relative radius (r/b) for abutment edge at L_c/L = 0.73 on local scour depth

The relative collar length of $L_c/L = 0.73$ is fixed around bridge abutment and the sharp edge of bridge abutment is changed to have a curvature shape with different radii (see Fig. 5). The edge shape of the abutment was changed to improve the flow field around the bridge support and hence more control to the local scour depth. The effect of different relative radii (r/b), of the abutment edge on local scour depth at bridge abutment was presented in Fig. 3. The relative radius of bridge abutment was changed to cover a wide range (r/b), i.e., (r/b = 0 (sharp edge), 0.2, 0.4, 0.6, 0.8, 1.0, 1.4, 2.4, 4.1 and 13.3). It was found that as the relative radius increases the local scour depth decreases and vice versa. In addition, the reduction percentages of local scour depth for r/b = 0 (sharp edge), 0.2, 0.4, 0.6, 0.8, 1.0, 1.4, 2.4, 4.1, and 13.3 are 69%, 87%, 88%, 90%, 92%, 93%, 94%, 95%, 96%, and 95.5% respectively, compared to the no-collar case for the present study

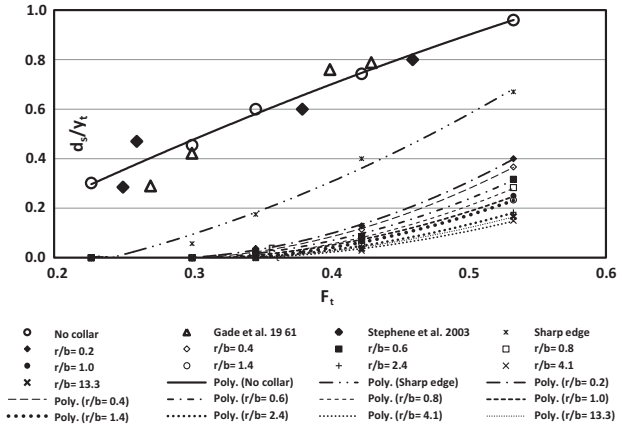

Figure 3 The relationship between d_s/y_t and F_t at different curvature radii of U.S. of abutment edge (r/b).

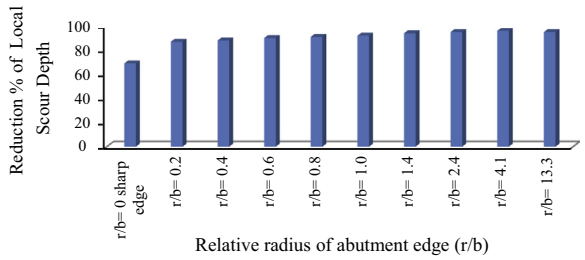

Figure 4 Reduction percentages of local scour depth for different r/b.

and the other studies [38,39], see Fig. 4. It is obvious that as the relative radius for abutment edge increases a well distribution for velocity around the obstacle will be attained and hence smaller values of local scour depth occurred around abutment. The scour contour maps for bridge abutment with r/b = 0.2, 0.6, 0.8, 1.0, 1.4, 2.4 and 4.1were presented in Fig. 5. This figure shows that, the scour hole dimensions for larger values of r/b are smaller compared to the smallest values of r/b. On the other hand, there are small scour holes formed downstream the bridge abutment, these scour holes will be controlled in the next section. Typical case for the time averaged velocity vectors is displayed for elevation at section A–A (Fig. 5) for r/b = 0.6 and 1.0 (Fig. 6a and b). It was shown that, flow velocity decreases as the r/b increases. Moreover, the intensity of circulatory motion is reduced for the larger values of r/b. The lateral time averaged velocity distribution just upstream the abutment nose was shown for r/b = 0.4, 1.0 and 2.4 Fig. 7. From this figure it is obvious that the distribution of flow velocity in lateral direction decreases as r/b increases. In

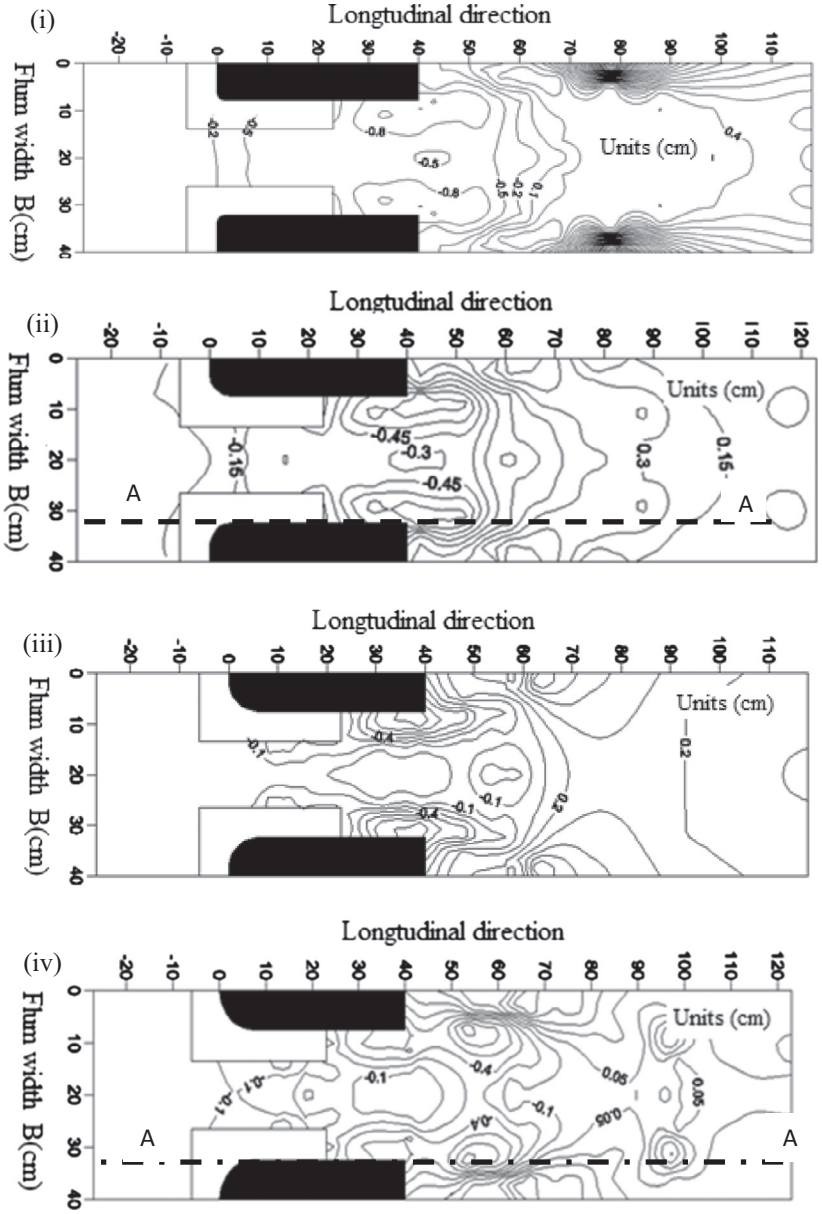

Figure 5 Scour contour maps for (i) r/b = 0.2, (ii) r/b = 0.6, (iii) r/b = 0.8 and (iv) r/b = 1.0 at Ft = 0.53.

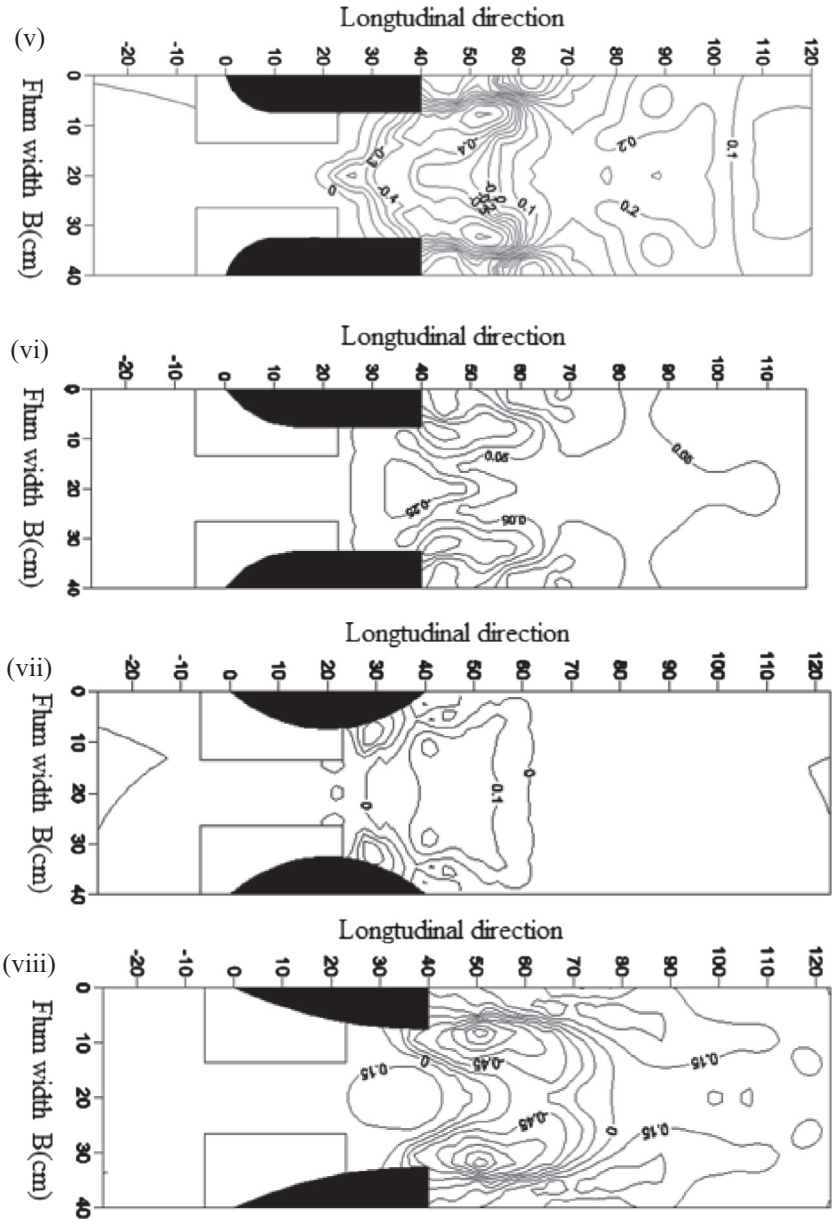

Fig 5. *(continued)*

addition, the measured profile of bed is observed to be close to the simulated ones using the computational fluid dynamic models. The simulated models for different values of r/b are compared to the measured data; the correlation coefficient and standard error are 96% and 5%, respectively Fig. 8.

5.2. Effect of collar length (L_c/L) for r/b = 4.1 on local scour depth

In the last section, the scour dimensions were reduced by more than 95%, but in the other side, two scour holes were formed downstream bridge abutment. So, it is an attempt to control these scour holes by changing the relative collar length for a typical case of r/b = 4.1. The collar length downstream of abutment was changed to have different relative lengths (L_c/L) = 1.3, 1.35, 1.4 and 1.45 with r/b = 4.1, to control the local scour depth downstream bridge abutment. The relationship between the maximum relative scour depth at bridge abutment (d_s/y_t) and the tail Froude number (F_t) for different relative lengths of collar was introduced in Fig. 9. It was found that at the relative length of collar 1.40, the local scour depth was vanished either for the upstream or for the downstream of the bridge abutment as shown in Fig. 10ii. It can be noticed that as the relative length of collar increases beyond the downstream of bridge abutment the more protection to the hydraulic structures. In which, as the collar length increases the down flow reduces. The local scour depth was

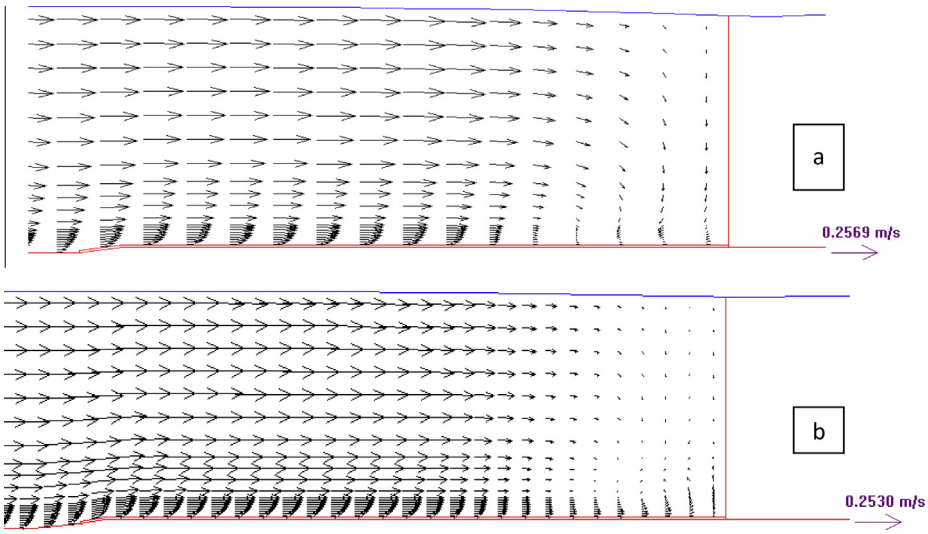

Figure 6 Time average velocity vectors for elevation cross-section A–A for (a) $r/b = 0.6$, (b) $r/b = 1.0$, (Fig. 5ii and iv, respectively).

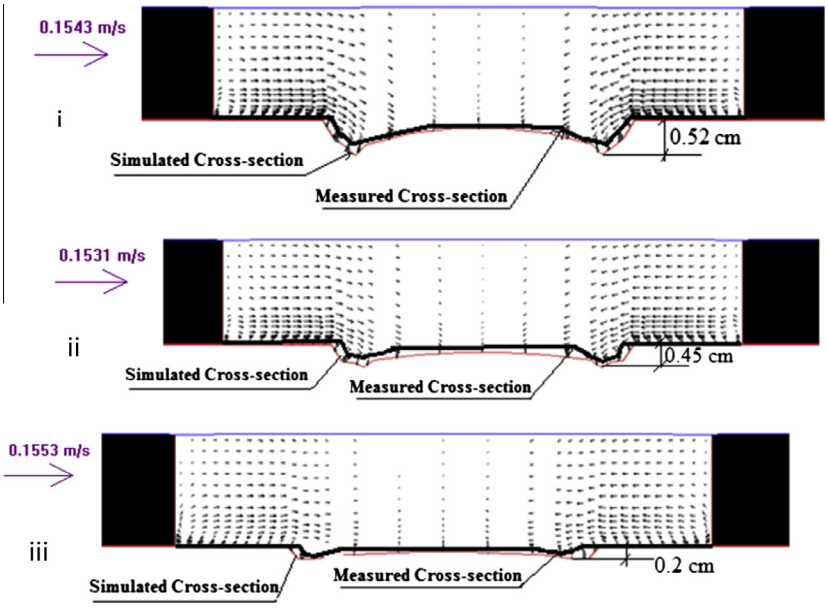

Figure 7 Time average velocity vectors for Lateral cross-section upstream the bridge abutment for (i) $r/b = 0.6$, (ii) $r/b = 1.0$ and (iii) $r/b = 2.4$ at $F_t = 0.42$.

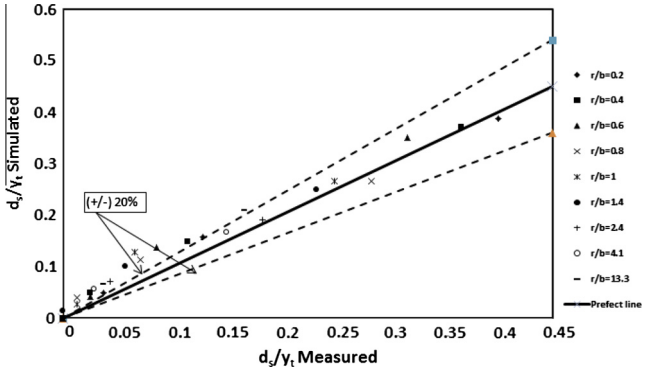

Figure 8 Simulated (d_s/y_t) versus experimental values for different r/b.

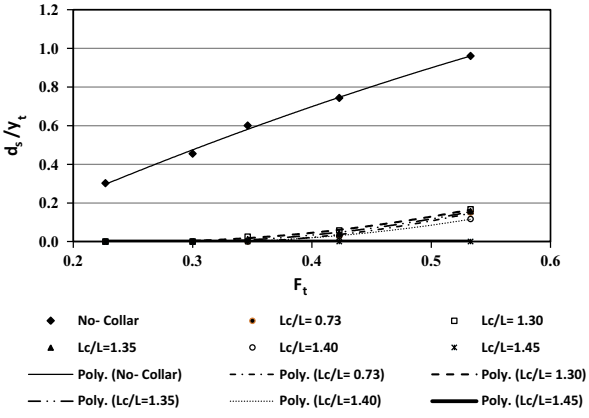

Figure 9 The relationship between d_s/y_t and F_t for different L_c/L and $r/b = 4.1$.

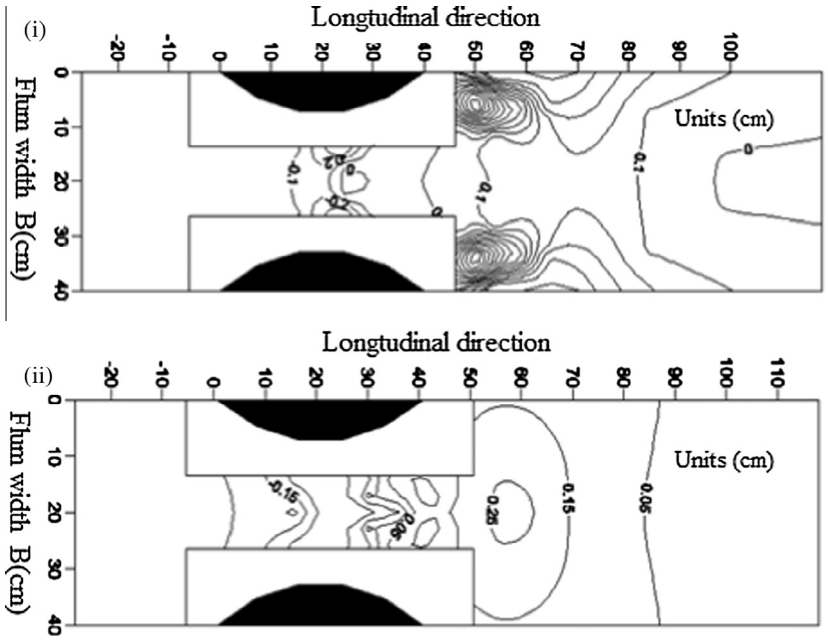

Figure 10 Scour contour maps for (i) $L_c/L = 1.3$ and (ii) 1.40 at $F_t = 0.53$.

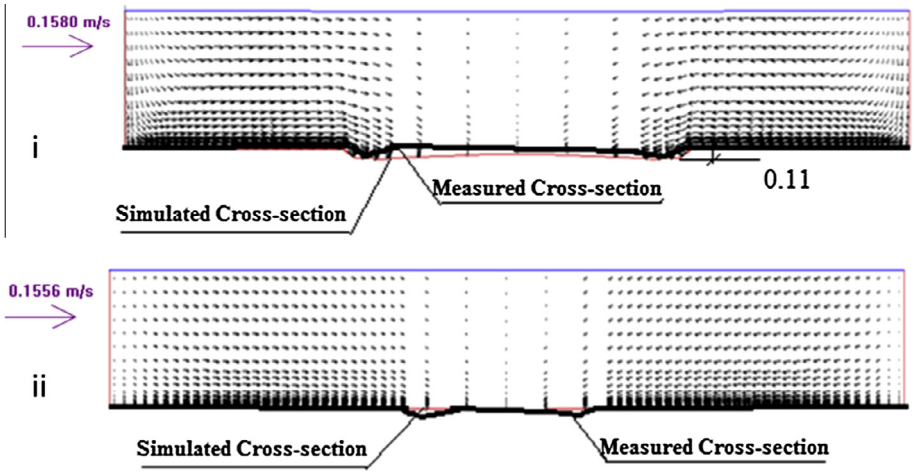

Figure 11 Time average velocity vectors for Lateral cross-section upstream bridge abutment for (i) $L_c/L = 1.3$ and (ii) $L_c/L = 1.45$ at $F_t = 0.42$.

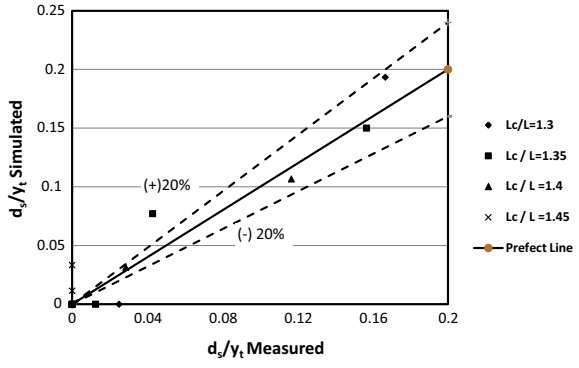

Figure 12 The simulated versus experimental values of d_s/y_t for different L_c/L.

reduced by 94%, 95%, 97%, and 100% for $(L_c/L) = 1.3$, 1.35, 1.4, and 1.45, respectively. The lateral time averaged velocity distribution just upstream the abutment nose was shown for $L_c/L = 1.30$, and 1.45 Fig. 11. From this figure it is obvious that the distribution of flow velocity in lateral direction decreases as L_c/L increases. In addition, the measured profile of bed is observed to be close to the simulated ones using the computational fluid dynamic models. The simulated models for different values of L_c/L are compared to the measured data; the correlation coefficient and standard error are 92% and 3%, respectively Fig. 12.

Photo 1 Re-circulating flume and experimental model.

6. Conclusions

In the present paper, experimental and numerical studies are implemented on a bridge abutment to simulate the local scour depth under the effect of changing the abutment edge shape and collar lengths. 3-D computational fluid dynamic models, which based on finite volume method to solve the Navier–Stokes equations, are created by using SSIIM program. It was found that, the relative scour depth decreases as the relative radius of abutment edge increases. In addition, the reduction percents of local scour depth for $r/b = 0$ (sharp edge), 0.2, 0.4, 0.6, 0.8, 1.0, 1.4, 2.4, 4.1, and 13.3 are 69%, 87%, 88%, 90%, 92%, 93%, 94%, 95%, 96%, and 95.5% respectively compared to the no-collar case. In addition, the increases of the relative length of collar share to more control and minimize the local scour depth either for upstream or for downstream of bridge abutment. Finally, the results of numerical models using SSIIM were found to be agreed well with the measured data for different experimental models.

References

[1] Richardson EV, Abed L. Top width of pier scour holes in free and pressure flow. Proceeding of international conference of hydraulic engineering, Part 1; 1993. p. 25–30.
[2] Parker GW, Bratton L, Armstrong DS. Stream stability and scour assessments at bridges in Massachusetts U.S. Geological survey open file Report No. 97-588 (CD-ROM). Marlborough, Mass.: Massachusetts Highway Dept. Bridge Section; 1997.
[3] Deng L, Cai CS. Bridge scour: prediction, modeling, monitoring and countermeasures, review. Practice Periodical Struct Des Construct 2010;15(2).
[4] Lagasse PF, Clopper PE, Zevenbergen LW, Girard LG. Countermeasures to protect bridge piers from scour. National cooperative highway research program (NCHRP) Rep. No. 593. Washington, D.C3: Transportation Research Board; 2007.
[5] Barkdoll BD, Ettema R, Melville BW. Countermeasures to protect bridge abutments from scour. National cooperative highway research program (NCHRP) Rep. No. 587. Washington, D.C.: Transportation Research Board; 2007.
[6] Li H, Kuhnle R, Barkdoll B. Spur dikes as an abutment scour countermeasure. Impacts Global Climate Change 2005:1–12.
[7] Sturm TW, Chrisochoides A. Abutment scour in compound channels for variable setbacks. Proc, Int Water Resour Eng Conf 1998:174–9. ASCE, Reston, VA.
[8] Melville BW, Coleman SE. Bridge scour. Highlands Ranch, CO.: Water Resources Publications; 2000.
[9] Richardson EV, Davis SR. Evaluating scour at bridges. Hydraulic engineering circular no. 18. 4th ed. Arlington, VA: Federal Highway Administration (FHWA); 2001.
[10] Sturm TW. Scour around bankline and setback abutments in compound channels. J Hydraul Eng 2006;132(1):21–32.
[11] Zarrati AM, Gholami H, Mashahir MB. Application of collar to control scouring around rectangular bridge piers. J Hydrauic Res, IAHR 2004;42(1):97–111.
[12] Zarrati AM, Nazariha M, Mashahir MB. Reduction of local scour in the vicinity of bridge pier groups using collars and riprap. J Hydraul Eng, ASCE 2006;132(2):154–62.
[13] Alabi PD. Time development of local scour at bridge pier fitted with a collar. Master degree thesis. Saskatoon, Saskatchewan, Canada: University of Saskatchewan; 2006.
[14] Moncada-M AT, Aguirre-Pe J, Bolivar JC, Flores EJ. Scour protection of circular bridge piers with collars and slots. J Hydraul Res 2009;47(1):119–26.
[15] Abdel-Aal GM, Mohamed YA. The effect of collar size and shape on scour depth around bridge piers. Sci Bull, Fac Eng 2010. Ain Shames University, Faculty of Engineering, Cairo, Egypt.
[16] Abdel-Aal GM, Mohamed YA, Waheed EO, El-fooly MM. Local scour mitigation around bridge piles using protective plate (collar). Sci Bull, Fac Eng 2008;2:343–54. Ain Shames University, Faculty of Engineering, Cairo, Egypt.
[17] Odgaard AJ, Wang Y. Scour prevention at bridge piers. In: Proceeding of hydraulic engineering national conference. Ragan, Virginia: ASCE; 1987. p. 523–7
[18] Chiew YM. Scour protection at bridge piers. J Hydraul Eng, ASCE 1992:1260–9.
[19] Grimaldi C, Gaudio R, Calomino F, Cardoso AH. Countermeasures against local scouring at bridge piers: slot and combined system of slot and bed sill. J Hydraul Eng, ASCE 2009:425–32.
[20] Gaudio R, Tafarojnoruz A, Calomino F. Combined flow-altering countermeasures against bridge pier scour. J Hydraul Res 2012;50(1):35–43.
[21] Tafarojnoruz A, Gaudio R, Dey S. Flow altering countermeasures against scour at bridge piers a review. J Hydrauic Res 2010:441–52.
[22] Tafarojnoruz A, Gaudio R, Calomino F. Bridge pier scour mitigation under steady and unsteady flow conditions. Acta Geophys 2011;60(4):1076–97.
[23] Fathi A, Zarrati A, Salamatian A. Scour depth at bridge abutments protected with a guide wall. Can J Civ Eng 2011;38(12):1347–54.
[24] Mowafy MH, Fahmy MR. The effect of constructing two adjacent bridges on the flow characteristics and local scour around bridge piers. Sci Bull, Fac Eng 2001;36(1):129–41. Ain shams university, Cairo, Egypt.
[25] Melville BW. Pier and abutment scour: integrated approach. J Hydraul Eng, ASCE 1997;123(2):125–36.

[26] Hua Li. Countermeasures against scour at bridge abutments. PhD Thesis. Michigan Technological University; 2005.
[27] Abou-Seida, Mostafa TMS, lsaeed GH, Elzahry EFM. Experimental investigation of abutment scour in sandy soil. J Appl Sci Res 2009;5(1):57–65, Faculty of Engineering (Shoubra), Benha University, Egypt.
[28] Kose O, Yanmaz MA. Scouring reliability of bridge abutments. Aksaray, Turkey: Aksaray University; 2010, Middle East Technical University, Ankara, Turkey, Published in Teknik Dergi, vol. 21, no. 1. p. 4919–34.
[29] Teruzzi A, Ballio F. Numerical investigation of the turbulent flow around a bridge abutment. River Flow– Ferreira, Alves, Leal & Cardoso; 2006.
[30] Pu JH, Lim SY. Efficient numerical computation and experimental study of temporally long equilibrium scour development around abutment. Environ Fluid Mech 2013.
[31] Şarlak N, Tiğrek Ş. Analysis of experimental data sets for local scour depth around bridge abutments using artificial neural networks. Water SA 2011;37(4).
[32] Mohammadpour R, Ghanib A, Azamathullac HM. Estimation of dimension and time variation of local scour at short abutment. Int J River Basin Manage 2013.
[33] Gaudio R, Grimaldi C, Tafarojnoruz A, Calomino F. Comparison of formulae for the prediction of scour depth at piers. Proc 1st European IAHR congress. Edinburgh, UK; 2010.
[34] Gaudio R, Tafarojnoruz A, De Bartolo S. Sensitivity analysis of bridge pier scour depth predictive formulae. J Hydroinformatics 2013;15(3):939–51.
[35] Tafarojnoruz A, Gaudio R. Discussion on scale effects in physical hydraulic engineering models. J Hydrauic Res, IAHR 2012;50(2):247–8, doi: 10.1080/00221686.2012.668377.
[36] Olsen NR. A three dimensional numerical model for simulation of sediment movements in water intakes with multiblock option. User's manual; 2007. <http://www.ntnu.no>.
[37] Van Rijn LC. Mathematical modeling of morphological processes in the case of suspended sediment transport. Ph.D. Thesis. Delft University; 1987.
[38] Garde RJ, Subramanya K, Nambudripad KD. Study of scour around spur-dikes. J Hydr Div Proc Am Soc Civ Eng 1961;87(6):23–37.
[39] Stephen EC, Christine SL, Melville B. Clear-water scour development at bridge abutments. J Hydrauic Res 2003;41(5):521–31.

Mr. Yasser A.M. Moussa received the M.Sc. and Ph.D. degrees in Civil Engineering Department from College of Engineering, Zagazig University, Egypt, in 2002 and 2005 respectively. During 2009, Dr Yasser Moussa was a Post Doctorate fellow with Hydroscience and Engineering, College of Engineering, University of Iowa, USA. Currently, he is an associate professor at college of engineering, Zagazig University, Egypt. His research interests are open channel hydraulics, stilling basins, sediment transport, simulation models, and artificial intelligence.

Mr. Tarek H. Nassralla received the M.Sc. degree in Civil Engineering Department from Benha Faculty of Engineering, Benha University, Egypt, in 2001 and Ph.D. degree in Civil Engineering Department from Faculty of Engineering, Minoufiya University, Egypt, in 2008. Currently, he is an Assistant Professor, Civil Eng Department, Benha University, Egypt. His research interests are open channel hydraulics, weeds, seepage, scour and irrigation development.

Mr. Gamal Mostafa received the M.Sc. and Ph.D. degrees in Civil Engineering Department from College of Engineering, Zagazig University, Egypt. His research interests are open channel hydraulics, stilling basins, sediment transport.

Mr. Ahmed SH.M. Awaad received the M.Sc. degree in Civil Engineering Department from College of Benha Engineering, Benha University, Egypt, in 2013.